Cumhuriyet Science Journal

e-ISSN: 2587-246X
ISSN: 2587-2680

Cumhuriyet Sci. J., 42(3) (2021) 694-701
http://dx.doi.org/10.17776/csj.927289

Effect of size modulation and donor position on intersubbands refractive index changes of a donor within a spherical core/shell/shell semiconductor quantum dot

***Emre Bahadir AL*[1,*]**

[1]*Sivas Cumhuriyet University, Faculty of Science, Department of Physics, Sivas/TURKEY*

Abstract

In the current study, linear, nonlinear and total relative refractive index changes of a single shallow hydrogenic donor atom confined in semiconductor core/shell/shell quantum dot heterostructure are investigated in detail by compact density matrix formalism. For this purpose, the energy eigenvalues and the corresponding wave functions are calculated by diagonalization method in the effective mass approximation. Then, intersubband $1s \rightarrow 1p$ and $1p \rightarrow 1d$ donor transition energies are calculated. In the study, the effects of core/shell sizes, donor position and depth of confinement potential are analyzed. The numerical results show that the linear and nonlinear refractive index changes undergo significant changes.

Article info

History:
Received:26.04.2021
Accepted:28.06.2021

Keywords:
Hydrogenic shallow donor impurity,
Quantum dots,
Optical transitions,
Refractive index,
Size effect.

1. Introduction

It is accepted that the progress of electronic and opto-electronic devices depends on understanding the basic chemical and physical properties of low-dimensional structures (LDSs). In these LDSs, the geometric confinement limits the movement of charge carriers in space and it causes major changes in electrical and optical properties due to the occurrence of discrete electronic energy distribution. Therefore, in recent years, intensive research activities have been conducted around the world on the behavior of matter at nanoscale. Although various devices have been devoted to nanoscale particles, the properties of controlled nanoscale materials such as light emitting diodes, photo detectors and quantum dot (QD) single photon source are still the biggest problem of scientists.

Due to the recent development of semiconductor nanoelectronics, it has become possible to reduce dimensionality from bulk semiconductors to zero-dimensional semiconductor nanostructures (QDs). These nanostructures are very important because their charge carrier motion is confined in three directions, and therefore efficient control of the physical properties of these structures becomes possible. Proper adjustment of the physical properties of QDs is advantageous because of their potential applications in the development of semiconductor optoelectronic devices. For this reason, some optical properties of semiconductor QDs such as dipole transition [1,2], oscillator strength [3,4], photoionization cross-sections [5], optical absorption coefficients (OACs) [6,7] and refractive index changes (RICs) [3,8] have attracted the attention of researchers in experimental and theoretical studies in recent years.

Since the electronic and optical properties in a QD are affected by the impurity, the physical properties related to impurity have been investigated using different methods such as variational approximation [5], tight-binding model [9], perturbation theory [10] and diagonalization method [6]. Some studies have revealed that it is possible to realize a single dopant scheme in QDs [11-13]. This enables the production of various optoelectronic devices.

Moreover, it should be noted that in the presence of the donor atom, calculating energy levels and wave functions is a difficult task that requires theoretical effort. In this case, it is very difficult to find analytical solutions. To overcome this difficulty, the calculation of the electronic state in the presence of donor atom will be done by the diagonalization method. It is hoped that this will allow a more detailed description of the impurity states in the structures under study.

*Corresponding author. *e-mail address: emrebahadiral@hotmail.com*

In theoretical studies, it is common to use spherical shaped QDs, and many researchers have focused on the optical properties of this type of structure [3,6,14-16]. Thanks to the rapid development of material growth techniques such as molecular beam epitaxy, metal-organic chemical vapor deposition and electron lithography and the advancement of chemical production processes, various dimensional new generation quantum nanostructures that allow electrons to be confined in these nanostructures have been produced, one of which is the coated spherical QDs called core/shell/shell QDs (CSSQDs) [17,18]. These structures consist of two semiconductors with different band gaps. They are spatially arranged in such a way that the larger bandwidth core acting as a substrate is covered by a smaller bandwidth spherical shells. The originality of these structures is that their physical properties can be adjusted in a controlled manner, leading to changes in energy levels. Therefore, it is important to study the electronic and optical properties of CSSQDs.

Previously, some studies on RICs of donor atom in spherical core/shell QDs have been published. The relative RICs as well as the OACs in the $GaAs/AlAs$ core/shell QD were calculated by M'zerd et al [19], considering the effects of presence of the donor atom and the donor position, as well as the interaction with the LO-phonon. Taking into account the effects of structure parameters, magnetic field and dielectric mismatch, Feddi et al [20] investigated the OACs and relative RICs for the $1s-1p$ transition of a single dopant confined in $AlAs/GaAs/SiO_2$ core/shell QDs. Linear and nonlinear intersubband OACs and RICs in $GaAs/AlGaAs$ core/shell spherical QDs were theoretically investigated by Zhang et al [21] for te cases with and without impurity at the center. The effect of pressure on the binding energy and the linear and nonlinear OACs and RICs associated with the intersubband transition of a dopant in an $AlAs/GaAs$ spherical core/shell QD, were studied by El Haouari et al [22].

However, there is no study in the literature on RICs caused by $1s \rightarrow 1p$ and $1p \rightarrow 1d$ single dopant transitions in the CSSQDs. Therefore, in the current theoretical study, the effect of the impurity position and confinement potential on the linear, nonlinear and total RICs of a single impurity atom in a CSSQD is numerically analyzed and discussed using density matrix formalism. As a result of this research, it has been shown that the RICs in CSSQD are strictly dependent on its geometric parameters and donor position.

2. Materials and Methods

2.1. Electron-impurity Hamiltonian and wave function

Since the optical behavior of nanoscale semiconductors is related to the electronic properties of the structure, the energy behavior of the confined donor must first be examined.

Consider a hydrogen-like shallow donor impurity located anywhere in the core region of a CSSQD nanocrystal with a spherically symmetrical $GaAs(core)/Al_{x_1}Ga_{1-x_1}As(inner\ shell)/Al_{x_2}Ga_{1-x_2}As(outer\ shell)$ design, where x_1 (x_2) is the aluminum concentration in the inner (outer) shell. GaAs core material with radius a_1 is covered with $Al_{x_1}Ga_{1-x_1}As$ shell, which has a wider band gap. $Al_{x_1}Ga_{1-x_1}As$ inner shell material with thickness $T_s = a_2 - a_1$ is covered with $Al_{x_2}Ga_{1-x_2}As$ shell which has a wider band gap ($x_2 > x_1$). In order to protect the nanostructure from contamination of the external environment, it is assumed that the structure is covered with a glass matrix. In the effective mass approximation, the Hamiltonian which describes the energy behavior of a single electron bound to the donor confined in such a system with a finite depth potential in the region $0 < r \leq a_1$, can be expressed as,

$$H = -\frac{\hbar^2}{2m^*}\nabla^2 + V(r) + V_C, \tag{1}$$

where the first term is the kinetic energy operator of the electron, $\hbar$ is the reduced Planck constant, m^* is the conduction band effective mass of the electron in the $GaAs$-core region, and ∇^2 is Laplacian in spherical coordinates.

The second term in Equation (1) represents the confinement potential. Due to the band gap difference between $GaAs$ ($E_g = 1.424\ eV$) and $Al_xGa_{1-x}As$ ($E_g = 1.424 + 1.247x\ eV$) [23], it is thought that the probability density will mostly be limited within the core region and the charge carriers will be confined within $GaAs$. It is a good approximation that the dielectric material outside the structure is considered to have an infinite potential barrier, and in this case it is possible to write the confinement potential in the form

$$V(r) = \begin{cases} 0, & r < a_1 \\ V_1, & a_1 \leq r < a_2 \\ V_2, & a_2 \leq r < a_3 \\ \infty, & r \geq a_3 \end{cases}, \tag{2}$$

where $V_{1,2} = 0.6\,(1247x_{1,2})\ meV$ is the conduction band offset between $AlGaAs$ and $GaAs$.

The third term in Equation (1) shows the Coulomb potential energy between donor impurity and electron and it has the form

$$V_C = -\frac{Ze^2}{\varepsilon|\vec{r}-\vec{r}_d|}, \quad (3)$$

where $Z = 0$ ($Z = 1$) corresponds to the case without (with) a hydrogenic donor impurity in the system, e is the charge of electron, ε is the dielectric constant, $|\vec{r}-\vec{r}_d|$ is the electron-impurity distance, $\vec{r}$ ($\vec{r}_d$) is the radial position of the electron (ionized donor) with respect to the center of the spherical QD. It is assumed that the ionized donor is placed along the z-axis. In terms of spherical harmonics $1/|\vec{r}-\vec{r}_d|$ term is given by [10]

$$\frac{1}{|\vec{r}-\vec{r}_d|} = \sum_\mu \frac{4\pi}{2\mu+1} f_\mu(r) \sum_{\upsilon=-\mu}^{\mu} Y^*_{\mu,\nu}(\theta,\phi) Y^*_{\mu,\nu}(\theta_d,\phi_d), \quad (4)$$

where $Y_{\mu,\nu}(\theta,\phi)$ are spherical harmonics, θ and ϕ (θ_d and ϕ_d) are the polar angles of the electron (impurity atom) and $f_\mu(r)$ is

$$f_\mu(r) = \begin{cases} \frac{1}{r_d}\left(\frac{r}{r_d}\right)^\mu, & r \le r_d \\ \frac{1}{r}\left(\frac{r_d}{r}\right)^\mu, & r \ge r_d \end{cases}. \quad (5)$$

At this point, in order to simplify numerical calculations, reduced units are used, defining $Ryd^* = \frac{m^* e^4}{2\hbar^2\varepsilon^2}$ as energy unit and $a_B^* = \frac{\varepsilon\hbar^2}{m^* e^2}$ as length unit. With these units, the Hamiltonian becomes in the form

$$H = -\nabla^2 + V(r) - 2Z\sum_\mu \frac{4\pi}{2\mu+1} f_\mu(r) \sum_{\upsilon=-\mu}^{\mu} Y^*_{\mu,\nu}(\theta,\phi) Y^*_{\mu,\nu}(\theta_d,\phi_d). \quad (6)$$

The solution of the Schrödinger equation $H\psi_{nlm}(r,\theta,\phi) = E_{nlm}\psi_{nlm}(r,\theta,\phi)$ is sought to determine the allowed energy levels and wave functions of the system, where, E_{nlm} is the electron energy eigenvalue for certain quantum numbers (n is the principal quantum number, l is the orbital quantum number, and m is the magnetic quantum number) and $\psi_{nlm}(r,\theta,\phi)$ is the wavefunction corresponding to this energy. The orbital quantum number $l = 0,1,2,...$ is marked by the usual notation $s, p, d, ...$ The diagonalization method will be used to solve this Schrödinger equation. For this purpose, the single electron wavefunctions of the infinite QD will be taken as the basis function:

$$\psi_{nlm}(r,\theta,\phi) = \sum_j c_{n_j}\psi^{(0)}_{n_j lm}(r,\theta,\phi), \quad (7)$$

where c_{n_j} are the expansion coefficients and $\psi^{(0)}_{n_j lm}(r,\theta,\phi)$ are the total wave functions describing the motion of the electron without the impurity atom. It should be remembered that the exact solutions for an electron in an infinite radial potential are [6]

$$\psi^{(0)}_{n_j lm}(r,\theta,\phi) = R^{(0)}_{nl}(r) Y_{l,m}(\theta,\phi), \quad (8)$$

where the radial wavefunction-$R^{(0)}_{nl}(r)$ is given as

$$R^{(0)}_{nl}(r) = \begin{cases} N j_l(k_{nl} r), & r < a_3 \\ 0, & r \ge a_3 \end{cases}, \quad (9)$$

where N is the normalization constant, k_{nl} is the nth root of the spherical Bessel function-j_l and a_3 ($a_3 >> a_2$) is the radius of the infinite spherical QD.

2.2. Linear, nonlinear and total RICs of the system

In a monochromatic electromagnetic field with a frequency ω, the probability of transition between states i and j is called as the oscillator strength-P_{ij} given by the Fermi golden rule and it is expressed in the form [22]

$$P_{ij} = \frac{2m^*}{\hbar^2} E_{ij} \left|M_{ij}\right|^2, \quad (10)$$

where, $E_{ij} = E_j - E_i$ is the energy difference, while M_{ij} is the dipole moment matrix element of the transition between the i and j states. The oscillator strength is highly dependent on the overlap of wave functions and the energy difference between states and thus it gives an idea of the dominant color of the emitted light.

Expressions of RICs can be obtained by density matrix approximation. Analytical expressions of linear and third order nonlinear sensitivities for a two-level quantum system are given in the forms

$$\chi^{(1)}_\omega(\omega) = \frac{\sigma_s \left|M_{ij}\right|^2}{\varepsilon_0(E_{ij} - \hbar\omega - i\hbar\Gamma_{ij})}, \quad (11)$$

and

$$\chi^{(3)}_\omega(\omega) = \frac{\sigma_s \hbar\omega |M_{ij}|^2 |\tilde{E}|^2}{\varepsilon_0(E_{ij} - \hbar\omega - i\hbar\Gamma_{ij})} \left[\frac{4\left|M_{ij}\right|^4}{\left(E_{ij} - \hbar\omega\right)^2 + \left(\hbar\Gamma_{ij}\right)^2} - \frac{\left|M_{jj} - M_{ii}\right|^2}{(E_{ij} - i\hbar\Gamma_{ij})(E_{ij} - \hbar\omega - i\hbar\Gamma_{ij})} \right], \quad (12)$$

where σ_s is the electron density in the system, ε_0 is the dielectric constant of the vacuum, ω is the angular frequency of light interacting with QD, $\hbar\omega$ is the incident photon energy, $\hbar\Gamma_{ij}$ is Lorentzian line width, $\Gamma_{ij} = 1 / T_{ij}$ is the non-diagonal damping term known as the relaxation ratio between the final and initial states, and it is defined as the inverse of the relaxation time-T_{ij}.

The sensitivity $\chi(\omega)$ is associated with the RIC in the form

$$\frac{\Delta n(\omega)}{n_r} = Re\left[\frac{\chi(\omega)}{2n_r^2}\right]. \quad (13)$$

Using Equations (11) and (12), linear and third order nonlinear RICs are obtained analytically in the form

$$\frac{\Delta n^{(1)}(\omega)}{n_r} = \frac{1}{2n_r^2\varepsilon_0}\frac{\sigma_s(E_{ij}-\hbar\omega)|M_{ij}|^2}{(E_{ij}-\hbar\omega)^2+(\hbar\Gamma_{ij})^2}, \quad (14)$$

and

$$\frac{\Delta n^{(3)}(\omega,I)}{n_r} = -\frac{\mu c I\sigma_s|M_{ij}|^4}{n_r^3\varepsilon_0}\frac{E_{ij}-\hbar\omega}{\left[(E_{ij}-\hbar\omega)^2+(\hbar\Gamma_{ij})^2\right]^2}\left[1 - \frac{|M_{jj}-M_{ii}|^2\left[E_{ij}^2-E_{ij}\left(\hbar\omega+\frac{(\hbar\Gamma_{ij})^2}{E_{ij}-\hbar\omega}\right)-2(\hbar\Gamma_{ij})^2\right]}{4|M_{ij}|^2\left[E_{ij}^2+(\hbar\Gamma_{ij})^2\right]}\right], \quad (15)$$

respectively, where $I = 2\varepsilon_0 n_r c\left|\tilde{E}\right|^2$ is the intensity of the linearly polarized electromagnetic field and μ indicates the magnetic susceptibility of the material. Thus, the total RIC is given as

$$\frac{\Delta n(\omega,I)}{n_r} = \frac{\Delta n^{(1)}(\omega)}{n_r} + \frac{\Delta n^{(3)}(\omega,I)}{n_r}. \quad (16)$$

Assuming that electromagnetic radiation is linearly polarized along the z-axis, the dipole moment matrix element is defined in a single electron system.by

$$M_{ij} = e\langle\psi_i|r\cos\theta\,|\psi_j\rangle, \quad (17)$$

where, ψ_i and ψ_j are wave functions of the initial and final states, respectively. In order for the dipole transition moment to be different from zero, the selection rules $\Delta l = \pm 1 \;\; and \;\; \Delta m = 0$ must be provided. Here, only the intersubband transitions between the $m = 0$ states of the CSSQD will be considered.

3. Results and Discussion

In this section, the effects of geometric confinement and change in donor position on RICs will be discussed according to the spherical CSSQD nanostructure model outlined above. The values of the material input parameters taken into account are presented as follows: $\varepsilon = 13.18, \quad m^* = 0.067m0 \quad (m_0 = 9.10956 \times 10^{-31}\,kg$ is the mass of the free electron), $I = 400\,MW/m^2, \quad \sigma_s = 1 \times 10^{23}\,m^3, \quad T_{ij} = 0.14\,ps$, $n_r = 3.2$, $a_B^* = 10.42\,nm$, $Ryd^* = 5.23\,meV$.

In Figure 1, the variation of linear, nonlinear and total RICs associated with $1s \rightarrow 1p$ and $1p \rightarrow 1d$ transitions is plotted as a function of photon energy for different core/shell sizes. The single donor is assumed to be located at the center of QD. As can be seen from the figure, the linear RICs increase with the photon energy and they reach a maximum value. Also, as can be seen from Equations 14 and 15, RICs are zero when $h\omega = E_{ij}$. When the core radius increases, the peaks of the RICs show a visible redshift (Figure 1 (a)). In addition, it is found that the increase in the peak amplitudes of the RICs is also associated with the increase in core size. Because the increase in the size of the core causes a decrease in the transition energy and an increase in the square of the non-diagonal electric dipole moment. It should also be noted that, due to the negative nonlinear term, the total RICs peaks get weaker compared to the linear response. The theoretical results reveal that the RICs associated with the $1p \rightarrow 1d$ transition have a significant decrease in the peak amplitudes with the increase in shell thickness, while the RICs associated with the $1s \rightarrow 1p$ transition are not affected by the shell thickness (Figure 1 (b)). Increasing shell thickness does not affect well-localized $1s$ and $1p$ electrons in the core region, while $1d$-level electron with greater energy than confinement potential-V_1 is localized in a larger region. In addition, it can be said that the nonlinear RICs are almost too weak. On the other hand, it is found that the peak positions of the RICs associated with the $1p \rightarrow 1d$ transition shift to red by increasing the shell thickness, but that the peak positions of the RICs associated with the $1s \rightarrow 1p$ transition are not affected by this increase.

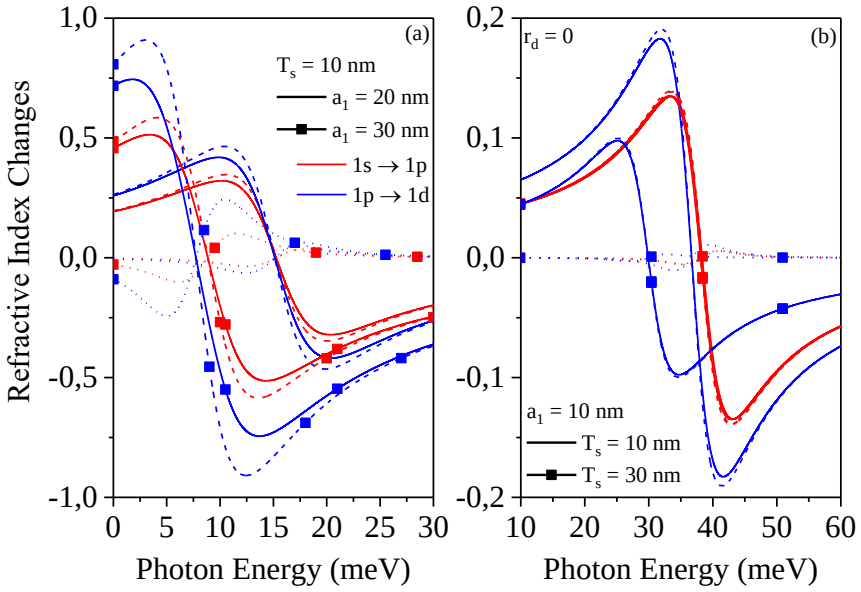

Figure 1. The variation of linear (dashed), third order nonlinear (dotted) and total (solid) RICs of $1s \rightarrow 1p$ and $1p \rightarrow 1d$ donor transitions for various core/shell sizes as a function of incident photon energy. The values are for $x_1 = 0.1$ and $x_2 = 0.4$.

In order to examine the effect of the intra-core position of the impurity atom on the on linear, nonlinear, and total RICs against the incident photon energy for the three important positions of the impurity are presented in Figure 2. For the $1s \rightarrow 1p$ transition, the peak amplitudes of the RICs increase as the impurity moves from the QD center to the core/shell boundary. The reason for this change is that as the impurity moves from the QD center to the core/shell boundary, the dipole matrix element increases as a result of better overlap of the wave functions of the respective states. However, due to the convergence of the $1s$ and $1p$ energy states, the peak positions of the RICs show a redshift as the impurity moves away from the QD center. Moreover, since the peak amplitudes of nonlinear RICs are very small compared to linear ones, the peak amplitudes of total RICs show an equivalent variation to linear ones. The same is true for the $1p \rightarrow 1d$ transition. However, as the impurity moves away from the QD center, the peak positions of the RICs for the $1p \rightarrow 1d$ transition shifts slightly towards blue and then red. This is because as the donor atom moves away from the QD center, the energy difference between the $1p$ and $1d$ states first increases and then decreases. Also, the peak amplitudes of the RICs increase due to the larger dipole matrix element at the core/shell boundary.

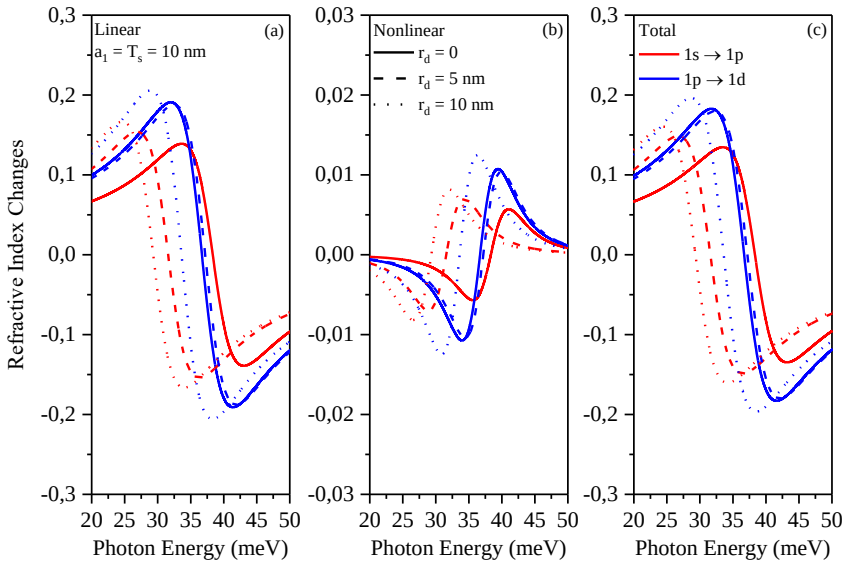

Figure 2. (a) Linear, (b) nonlinear and (c) total RICs related to $1s \rightarrow 1p$ and $1p \rightarrow 1d$ donor transitions against incident photon energy for $a_1 = T_s = 10\ nm$ and three impurity position values. The values are for $x_1 = 0.1$ and $x_2 = 0.4$.

Finally, RICs as a function of photon energy for different x_1 concentrations are presented in Figure 3. The figure shows that increasing x_1 concentration shifts the peak positions of RICs to blue. This is because the transition energy increases due to the quantum size effect with increasing x_1 concentration. In addition, it is found that the peak amplitudes of RICs monotonously decrease with increasing x_1 concentration. This is because the coincidence of the wave functions of the states of interest decreases as the x_1 concentration increases.

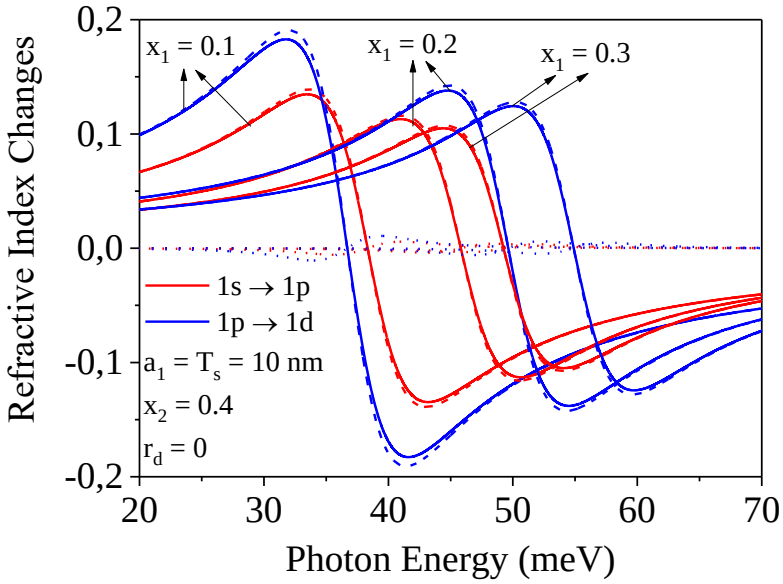

Figure 3. Linear (dotted), third-order nonlinear (dashed) and total (solid) RICs associated with $1s \rightarrow 1p$ and $1p \rightarrow 1d$ central donor transitions as a function of photon energy for various x_1 concentrations.

In conclusion, in the current theoretical study, the linear, nonlinear and total RICs of a single donor impurity atom confined within the spherical $GaAs(core)/Al_{x_1}Ga_{1-x_1}As(inner\ shell)/Al_{x_2}Ga_{1-x_2}As(outer\ shell)$ type CSSQD are extensively investigated, taking into account the

effects of core/shell sizes, donor position and depth of confinement potential. The results obtained show the following: The increase in core size increases the peak amplitudes of the RICs and shifts the peak positions to red. While the increase in shell thickness is not affect the peak amplitudes and peak positions of RICs related to the $1s \rightarrow 1p$ transition, it decreases the peak amplitudes of the RICs related to the $1p \rightarrow 1d$ transition and shifts the peak positions to red. As the impurity moves from the QD center towards the core/shell boundary, the peak amplitudes of the RICs of the $1s \rightarrow 1p$ transition increase and the peak positions shift to red. For the $1p \rightarrow 1d$ transition, as the impurity moves away from the QD center, the peak positions of the RICs shift to blue and then to red, and the peak amplitudes first decrease and then increase. Increasing x_1 concentration leads to a deeper confinement potential, and as a result, the peak amplitudes of the RICs decrease while the peak positions shift to blue. As a result, the theoretical results obtained here may contribute to experimental studies and offer a good model for practical applications such as optoelectronic devices and optical communication.

Acknowledgment

This work is supported by the Scientific Research Project Fund of Sivas Cumhuriyet University under the project number F-2021-641.

Conflicts of interest

The author state that did not have conflict of interests.

References

[1] Hasanirokh K., Asgari A., Rokhi M. M., Theoretical study on nonlinear optical properties of CdS/ZnS spherical quantum dots, *Optik*, 188 (2019) 99-103.

[2] Safeera T. A., Anila E. I., Synthesis and characterization of ZnGa2O4:Eu3+ nanophosphor by wet chemical method, *Scripta Mater.*, 143 (2018) 94-97.

[3] Naimi Y., Comment on "Magnetic field effects on oscillator strength, dipole polarizability and refractive index changes in spherical quantum dot", *Chem. Phys. Lett.*, 767 (2021) 138380.

[4] Sakr M. A. S., Gawad S. A. A., El-Daly S. A., Kana M. T. H. A., Ebeid El-Zeiny M., Photophysical and TDDFT investigation for (E, E)-2, 5-bis [2-(4-(dimethylamino)phenyl) ethenyl]pyrazine (BDPEP) laser dye in restricted matrices, *J. Mol. Struct.*, 1217 (2020) 128403.

[5] Shi L., Yan Zu-Wei, Meng Mei-Wen, Binding energy and photoionization cross section of hydrogenic impurities in elliptic cylindrical core/shell quantum dots under a non-axial electric field, *Superlattice Microst.*, 150 (2021) 106818.

[6] Al E. B., Kasapoglu E., Sari H., Sökmen I., Optical properties of spherical quantum dot in the presence of donor impurity under the magnetic field, *Physica B*, 613 (2021) 412874.

[7] Mgidlana S., Şen P., Nyokong T., Direct nonlinear optical absorption measurements of asymmetrical zinc(II) phthalocyanine when covalently linked to semiconductor quantum dots, *J. Mol. Struct.*, 1220 (2020) 128729.

[8] Yu D., Yu Z., Zhang Y., Chang Y., Yu D., Cation-exchange synthesis and measurement of PbS quantum dots with high nonlinear optical properties, *Optik*, 210 (2020) 164509.

[9] Pérez-Conde J., Bhattacharjee A. K., Electronic structure and impurity states in GaN quantum dots, *Solid State Comm.*, 135 (2005) 496-499.

[10] Yakar Y., Çakır B., Özmen A., Off-center hydrogenic impurity in spherical quantum dot with parabolic potential, *Superlattice Microst.*, 60 (2013) 389-397.

[11] Mocatta D., Cohen G., Schattner J., Millo O., Rabani E., Banin U., Heavily doped semiconductor nanocrystal quantum dots, *Science*, 332 (2011) 77-81.

[12] Koenraad P.M., Flatté M.E., Single dopants in semiconductors, *Nat. Mater.*, 10 (2011) 91-100.

[13] Moraru D., Udhiarto A., Anwar M., Nowak R., Jablonski R., Hamid E., Tarido J.C., Mizuno T., Tabe M., Atom devices based on single dopants in silicon nanostructures, *Nanoscale Res. Lett.*, 6 (2011) 479-487.

[14] Máthé L., Onyenegecha C. P., Farcaş A. -A., Pioraş-Ţimbolmaş L. -M., Solaimani M., Hassanabadi H., Linear and nonlinear optical properties in spherical quantum dots: Inversely quadratic Hellmann potential, *Phys. Lett.*, 397 (2021) 127262.

[15] Naifar A., Zeiri N., Nasrallah S. Abdi-Ben, Said M., Linear and nonlinear optical properties of CdSe/ZnTe core/Shell spherical quantum dots embedded in different dielectric matrices, *Photonics and Nanostructures*, 40 (2020) 100789.

[16] Al E. B., Kasapoglu E., Sakiroglu S., Sari H., Sökmen I. Duque C. A., Binding energies and optical absorption of donor impurities in spherical quantum dot under applied magnetic field, *Physica E*, 119 (2020) 114011.

[17] Dorfs D., Hickey S., Eychmüller A., Type-I and Type-II core-shell quantum dots: Synthesis and characterization, *Kumar CSSR (Ed) Semiconductor Nanomaterials, Weinheim: Wiley-VCH*, (2010) 331-366.

[18] Maximov M. V., Asryan L. V., Shernyakov Yu. M., Tsatsul'nikov A. F., Kaiander I. N., Nikolaev V. V., Kovsh A. R., Mikhrin S. S., Ustinov V. M., Zhukov A. E., Alferov Zh. I., Ledenstov N. N. Bimberg D., Gain and threshold characteristics of long wavelength lasers based on InAs/GaAs quantum dots formed by activated alloy phase separation, *IEEE J. Quant. Electron.*, 37 (2001) 676-683.

[19] M'zerd S., El Haouari M., Talbi A., Feddi E., Mora-Ramos M. E., Impact of electron-LO-phonon correction and donor impurity localization on the linear and nonlinear optical properties in spherical core/shell semiconductor quantum dots, *J. Alloy. Comp.*, 753 (2018) 68-78.

[20] Feddi E., Talbi A., Mora-Ramos M. E., Haouari M. El, Dujardin F., Duque C. A., Linear and nonlinear magneto-optical properties of an off-center single dopant in a spherical core/shell quantum dot, *Physica B*, 524 (2017) 64-70.

[21] Zhang Zhi-Hai, Zhuang G., Guo Kang-Xian, Yuan Jian-Hui, Donor-impurity-related optical absorption and refractive index changes in GaAs/AlGaAs core/shell spherical quantum dots, *Superlattice Microst.*, 100 (2016) 440-447.

[22] El Haouari M., Talbi A., Feddi E., El Ghazi H., Oukerroum A., Dujardin F., Linear and nonlinear optical properties of a single dopant in strained AlAs/GaAs spherical core/shell quantum dots, *Optic. Comm.*, 383 (2017) 231-237.

[23] Adachi S., GaAs, AlAs, and $Al_xGa_{1-x}As$: Material parameters for use in research and device applications, *J. Appl. Phys.*, 58 (1985) R1-R29.